VACUUM PRESSURE OBSERVATIONS DURING 2011 PROTON RUN

G. Bregliozzi, G. Lanza, V. Baglin, J.M. Jimenez

CERN, Geneva, Switzerland

Abstract

During the 2011 LHC proton run, different dynamic vacuum effects were detected and analysed in the LHC: electron cloud, synchrotron radiation, pressure spikes and beam induced heating effects. Electron clouds (EC) build up and pressure rises were measured with different bunch spacings and in different positions of the LHC. After a scrubbing run period performed in April 2011, the secondary electron yield of the vacuum surfaces was reduced to a level so that the EC effect was not anymore a limiting factor for the operation. Pressure spikes during injection, energy ramp and stable beams were observed mainly in LSS2 and LSS8 and in some cases lead to beam dumps. Beam induced heating effects were detected in different locations of the accelerator, mainly in TDI, MKI and TCP collimators in LSS7. This paper reviews all these observations and summarizes the mitigation solutions deployed for each location during the Winter Technical Stop (WTS) 2011-2012.

ELECTRON CLOUD EFFECT

The build up of the Electron Cloud (EC) and consequently the pressure rise due to the electron multipacting was observed for the first time in LHC during 2010. It occurred where both beams circulate in the same aperture with 150 ns bunch spacing proton beams. When decreasing the bunch spacing to 75 ns and finally to 50 ns, the EC effect was amplified and observed, as expected, all along the room temperature vacuum beam pipes, except on NEG coated beampipes. During the process, the electrons generated by the beam ionization of the residual gas, are accelerated towards the vacuum chamber wall by the electric field of the successive bunches. When impinging onto the vacuum chamber walls, these electrons generate secondary electrons which build up into a cloud [1-2]. The signature of electron cloud was a fast pressure increase due to electron stimulated desorption. It occurred at specific location where beam components as seen by the beams, were not NEG coated. Dedicated studies were then performed with 50 ns bunch spacing so as to define the building up parameters and to better understand these pressure increases [3].

Figure 1 shows the averaged pressure increase for two LHC typical areas observed during the injection of bunches with 50 ns bunch spacing at 450 GeV. Fast pressure rise are observed after each injection.

The highest pressure rise was measured at vacuum gauges installed on unbaked cold-warm transition. At that position, as shown in Figure 2A, the pumping speed resulted from the combination of upstream (from left to right) the NEG vacuum chambers (ϕ 80 mm) and of the downstream cold beam screen (ϕ 52 mm). One ion pump is also present in the module. The length of the uncoated part is of 1.3 m.

The lowest pressure rise was measured at vacuum gauges installed on baked vacuum module. As shown in Figure 2B, the pumping speed is obtained by the NEG vacuum chambers (ϕ 80 mm) which are installed on both sides of the vacuum gauge. The length of the uncoated parts is of 0.3 m, 4 times less than in the previous case. The closest ion pump for this type of layout configuration is at 7 m and provides a maximum effective pumping speed for methane (CH_4) of 10 L/s.

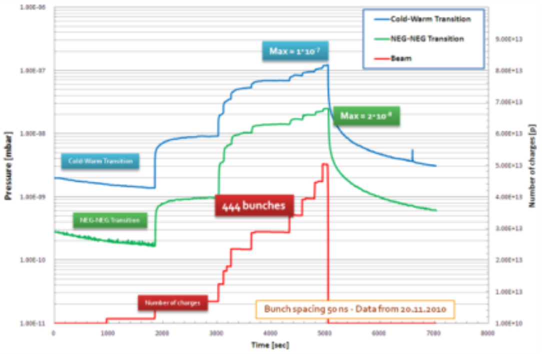

Figure 1: Pressure rise observed with 50 ns bunch spacing proton beams for the two types of layout configurations existing in the LHC machine.

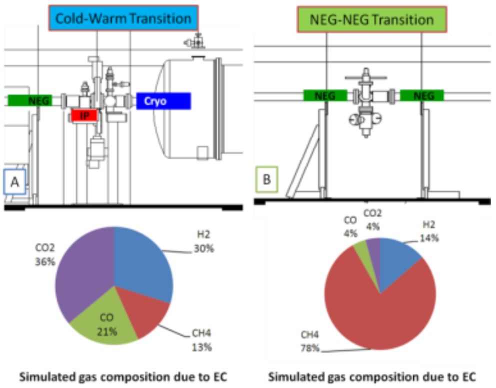

Figure 2: Sketch of the two typical layout configurations with the different pumping available at the level of the gauge (cryogenic, NEG and ion pumps) and with the estimated gas composition in presence of an electron cloud.

The VASCO code [4] was used to determine the gas composition at the level of the gauges shown in Figure 2. The measured pressure increase due to the EC effect is dependent on the desorption yield (η_{Gas}), the electron flux ($\dot{\Gamma}$) and the effective pumping speed (S_{effGas}) at the level of the pressure gauge, as indicated in (1).

$$P_{Gas} \approx \frac{\eta_{ElectronGas} \cdot \dot{\Gamma}_{Electron}}{S_{EffGas}} \qquad (1)$$

Assuming that $\dot{\Gamma}$ is the same all along the beam pipes, the pressure difference between configurations A & B depends only on the different effective pumping speeds for each single gas available at the port of the vacuum gauge and of the cleanliness of the surface. Thus, the pressure increase at configuration B is mainly due to CH_4, gas not pumped by the NEG coating, whereas at configuration A, due to the presence of different kind of pumping mechanism, the pressure increase is mainly due to CO_2 and H_2.

By design, vacuum cleaning and beam scrubbing is the mitigation for the electron multipacting problem. The vacuum cleaning is a dose effect due to the electron bombardments which produce a decrease of the electron desorption yield, η, and so the number of gas molecules desorbed from the surface of the beam vacuum pipe by the incident electron. The beam scrubbing is also a dose effect due to the electron bombardments but in that case produces a reduction of the secondary electron yield, δ, and so the number of secondary electron generated by the incident electron.

In April 2011, during a dedicated scrubbing run with 50 ns bunch spacing, clear evidence of vacuum cleaning was observed all around the machine. The decrease of the dynamic pressure function of the beam time of a cold warm transition is shown in Figure 3. After about 28h of vacuum cleaning and beam scrubbing, a pressure decrease of one decade was measured. Dedicated simulation study based on the recorded pressure data in the NEG-NEG transition (stainless steel bellow module with copper RF fingers and inserts) showed that the δ has decreased from about 1.9 to roughly 1.6 during this scrubbing run [5,6].During the physic operation at 50 ns, a further cleaning and scrubbing was then performed and before starting injection of 25 ns beams into the LHC, the δ_{max} in the different regions had reached values very close to the thresholds for electron cloud build up with 50 ns beams.In October 2011, a first beam injection with 25 ns bunch spacing was performed. A proton beam with an average intensity of $8 \cdot 10^{+10}$ p/b was injected at 450 GeV. Figure 4 shows the pressure increase in the two typical locations of the accelerator. Thanks to the conditioning obtained during the scrubbing run and the 50 ns physic run, an injection up to 2100 bunches with a total pressure increase well below the interlock level of the vacuum sector valves ($P_{MAX} < 1 \cdot 10^{-7}$ mbar) was achieved.

The comparison of the data in figure 1 and 4 allows different conclusions. The NEG-NEG transition (configuration B) of the LHC is almost fully scrubbed and conditioned and is not anymore a limiting factor for the LHC performance for further beam with 25 ns bunch spacing at higher intensity. Similarly, the cold-warm transition in configuration A must be also almost fully scrubbed during the 2011 LHC run and therefore should not present a limitation for the LHC performances too. However, electron flux, and therefore conditioning rate, between field free and field regions are significantly different. Therefore, electron clouds do not appear at the same time at all location of the LHC [7]. With 25 ns bunch spacing the induced heat load due to electron clouds in the bending magnets or stand alone magnets, previously not significantly scrubbed, was sufficient to desorbs molecules form the cryogenic area. Thus, the pressure increase recorded in configuration B is now dominated by gas desorption from the beam screen.

For a future beam operation with 25 ns bunch spacing at higher intensity, an additional scrubbing time is necessary so as to decrease the dynamic pressure coming from the cryogenic area, as well as to decrease beam coherent instabilities and incoherent emittance growth of the proton beam [8].

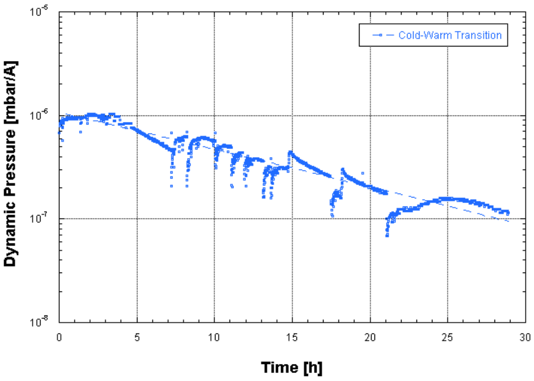

Figure 3: Dynamic pressure variation function of scrubbing time.

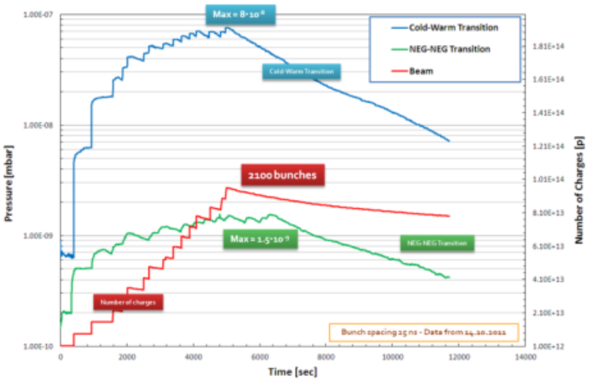

Figure 4: Pressure rise with 25 ns bunch spacing proton beam for the two different configurations of the machine.

SYNCHROTRON RADIATION

The first signs of synchrotron radiation (SR) were observed at the arc extremities during summer 2010. At that time, it was clearly identified that, at flat top, one beam pipe showed a pressure increase in the range of a few 10^{-10} mbar for some mA while the other one, at the same location, did not show any. In all cases, the pressure rise was correlated with the proton beam which was coming out of the arc. Since then, the beam current has increased to 320 mA (fill 2040) with a pressure increase at the arc extremity of 10^{-9} mbar. At the end of the year, the accumulated photon dose in the arc is about 10^{23} ph/m.

Figure 5 shows the dynamic pressure increase in mbar/A measured at the arc extremity as a function of the integrated photon dose, Γ. The molecular desorption yield, η, proportional to the dynamic pressure, is reduced according to (2). α is equal to 0.7 which is closed to values observed in other machines [9].

$$\eta \propto \Gamma^{-\alpha} \qquad (2)$$

After the beam injection with 25 ns bunch spacing, at the end of the year, a further decrease of the dynamic pressure function of the photon dose could be detected.

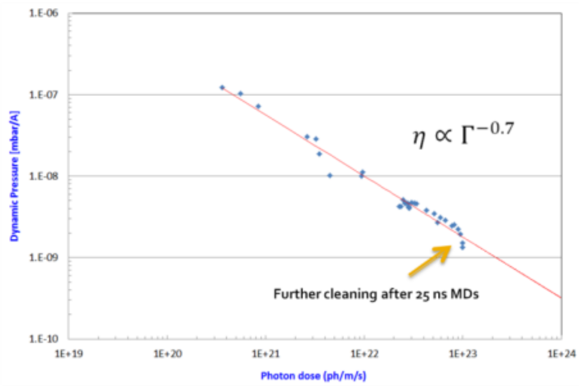

Figure 5: Reduction of the dynamic pressure measured at the arc extremity versus the photon dose.

PRESSURE SPIKES IN LSS2 AND LSS 8

During the 2011 LHC operation, several beam dumps were due to pressure spikes taking place in vacuum sectors located in the LSS2 and LSS8 where the two LHC beams circulate in a common beam pipe, namely vacuum sectors A4L2, A4R2, A4L8 and A4R8. Figure 6 shows an example of typical pressure spikes observed in LSS8. They appeared during beam injection, energy ramp and stable beam mode. X-ray imaging of all the bellows located in the concerned vacuum sectors was done. This work was part of a global campaign of bellows imaging launched during WTS 2010-2011. It must be stressed that vacuum sectors A4L2 and A4R2 were analysed and in May 2011 and all the bellows modules were found conform. Figure 7 shows a typical X-ray image of a VMTSA module from vacuum sectors A4L2, A4R2, A4L8 and A4R8 taken in September 2011. The module is non-conform with RF fingers no longer in contact with the insert. This non-conformity is due to the circulation of intense proton beams. When the beam circulates in these vacuum sectors, electric sparks could be generated between the non-contact RF fingers and the insert, causing the pressure spikes. The VMTSA is a special double bellow module, 780 mm length, installed beside the TCTVB, TCLIA and TCDD equipment to allow the movement of collimators along their 5th axis. The opening shape is elliptical with H70, V180 axis.

During WTS 2011-2012, the four vacuum sectors were vented, opened and all VMTSA removed and analysed. These investigations have shown that the stainless steel spring, installed around the RF fingers and designed to keep them in contact with the insert, have been subjected to plastic deformation and even brazing to the RF fingers. Moreover, some RF fingers were also permanently deformed. In order to produce plastic deformation and brazing an estimated temperature of more than 800°C could have been reached during operation.

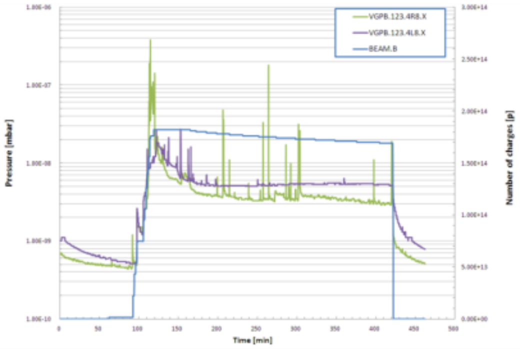

Figure 6: Dynamic pressure observed during injection, ramp and stable beam in LSS8 (31/10/2011).

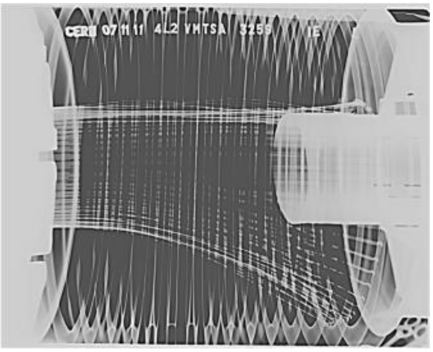

Figure 7: X-ray image of the RF fingers in the VMTSA bellow module.

Laboratory investigations with a network analyser on a spare module have shown that a resonance inside the bellow module is measured at 650 MHz *i.e.* within the LHC bunch spectrum. This resonance seems to be due to the cavity located behind the RF bridge coupled through the bad contacts of the RF fingers. During operation, it could lead to power dissipation in the RF fingers and spring of ~ 1W and causing a temperature increase [10].

All VMTSA modules installed in the LHC were modified during the WTS 2011-2012 *i.e.* 8 components (16 inserts in total). As the length of the RF fingers was shortened to improve the electrical contact, from ~ 170 mm to 50 mm, the movement along the 5th axis of TCTVB, TCLIA and TCDD is no longer allowed and must be blocked [11]. Additionally ferrite pieces are installed in each module so as to absorb the dissipated power and prevent any damage of the spring and RF fingers. Figure 8 shows the final assembly of the new VMTSA module. The acceptance tests from the RF tests are still ongoing and possible modification of the design could be applied in order to improve further the design.

Figure 8: New assembly of the VMTSA module with the ferrite blocks.

HEATING EFFECTS

During the LHC 2011 run, beam induced heating were recorded in different areas of the accelerator such as MKI injector kickers (LSS2&8), TDI injection (LSS2&8) collimators and TCP primary collimators in LSS7.

Figure 9 shows an example of temperature evolution in the MKI located in LSS8 during the whole year 2011. The temperature increases up to 60°C while the beam intensity and number of bunches increase throughout the year. At the same time a pressure increase was detected all around these locations of the accelerator. This temperature increase enhances a gas thermal outgassing as described by (3)

$$q = q_0 e^{-(\frac{E}{kT})} \tag{3}$$

The outgassing molecules are pumped by the vacuum activated NEG coating present in the area, and depending on the desorption rate, could cause its saturation. As a function of this saturation process, possible vacuum re-activations could be foreseen during LHC run 2012. An estimated time of 10 days, depending on the length and complexity of the vacuum sector, must be allocated for this kind of operation.

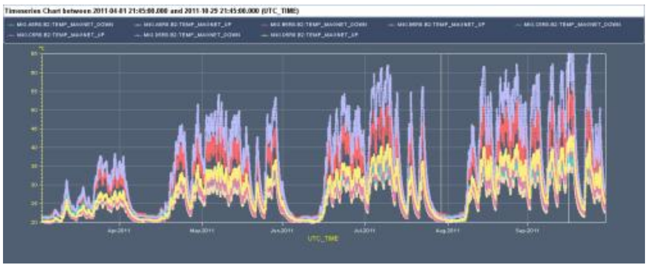

Figure 9: Temperature increase during 2011 in the MKI located in LSS8 [12].

CMS PRESSURE SPIKES

Unexpected pressure spikes, localized at 18.3 m on the right side of CMS interaction point (IP), appeared from time to time during 2011 physic run. In some cases, the high background due to the pressure increase (up to 10^{-6} mbar), did not allow CMS to take data. During WTS 2011-2012, X-ray imaging of the forward module located at 18.3 m from the IP shows a non-conform RF insert. The origin of this non conformity, overrunning the maximum allowed installed length of the module, is still under investigation. Following the imaging, it was therefore decided to exchange the RF insert inside the module. This operation normally requires an air venting of the NEG coating in the IP with a consequent need of a full bake-out and activation of the vacuum chambers in the CMS vacuum sector. Since a full bake-out of CMS requires the complete opening of the detector, this approach was discarded due to time constraints. It was decided to proceed to the exchange of the RF insert under a constant flow of pure neon [13]. The used neon venting system allows the mechanical interventions while preventing the saturation of the activated NEG coating. The principle is to over-pressurize the vacuum beam pipes with a gas which is not pumped by NEG, remove the faulty component and then pump down the sector again. The over-pressurization of such a gas in the vacuum sector prevents the NEG from saturation during the exchange of the faulty component, thus avoiding air back streaming through the beam pipe aperture.

The main steps of the working sequence are: fill the beam pipe with ultra pure neon with an initial overpressure of 200 mbar above atmosphere prior to the intervention, open the module with the non-conform RF insert while flushing ultra pure neon through the beam pipes, exchange the RF-contact and re-install the module followed by a pump-down and partial bake-out and re-activation of the NEG [14].

The exchange intervention in CMS was performed on January 18th. After a first pump down of about 48h the pressure in the IP was in the 10^{-9} mbar range. This result confirms the good development of the intervention and assures that the NEG vacuum chambers are still pumping. On January 24th, the partial bake-out of the area started [15]. After 24h at room temperature, the final pressure all along the beam pipes in the interaction point of CMS is in the low 10^{-10} mbar. Therefore, this intervention allowed the repair of the faulty RF insert and the restoration of the

CMS vacuum properties. Additional, X-rays imaging of all the bellow modules with RF fingers was performed after the bake-out and confirms their proper mechanical installation. Finally, transmission measurements along the CMS vacuum sector demonstrated that the NEG performances at the level of the interaction point were not significantly altered after the intervention [16].

LSS2 MODIFICATIONS

The ALICE Zero Degree Calorimeter (ZDC) system, situated in the LHC tunnel at a distance of about 114 meters upstream and downstream of the ALICE IP, is an integral part of the ALICE experiment. A TCTVB placed upstream to the ZDC at 73m from IP2 and partially shadowing the detector, has a very strong impact on the ZDC performance. A technical solution for the problem consists in reproducing the same collimation layout as in LSS1 and LSS5, *i.e* moving the recombination chamber by 1.36 m towards IP2 to install a TCTVA between the recombination chamber and D2. The venting of the vacuum sector with the insertion of new vacuum chambers will require a partial reconditioning under electron bombardment. During this phase, the background to ALICE could be larger than achieved during LHC run 2011. However this drawback was considered acceptable by the ALICE collaboration [17].

The two vacuum sectors, after N_2 venting and mechanical installation, were reinstalled with the new proposed layout. A complete bake-out and NEG vacuum activation of the sector is performed during week 5 and 6 of 2012 and the static pressure of the sector will be restored. Furthermore, venting and re-baking this area has produced an increase in the secondary electron yield of all the uncoated parts and could lead to an increased e-cloud effect and in turn, pressure increase. Vacuum scrubbing and conditioning of this area with a 50 ns bunch spacing protons beam could be done during the commissioning period if the bunch intensity is high enough ($>1.2 \cdot 10^{11}$ p/b), and this, without any need of a dedicated scrubbing run. Additionally, solenoids are installed in the extremities of the ID800 ZDC vacuum chambers and at the cold-warm transitions between D1 and D2, thus allowing if necessary, the electron multipacting reduction.

CONCLUSIONS

The 2011 operation with high intensity proton beam at 50 ns evidenced the efficiency of the vacuum cleaning and scrubbing with electron multipacting suppression.

For the 2012 operation, two distinctive scenarios could be foreseen for the electron cloud suppression:

1) Operation with 50 ns bunch spacing

The scrubbing run performed in April 2011 and following physics fill allowed injection of up to 1380 bunches with a maximum bunch intensity of $\sim 1.45 \cdot 10^{11}$ p/b without any significant pressure increase due the electron cloud effect. After the mechanical repairs performed during the WTS 2011-2012, 10 vacuum sectors were vented to air, subsequently re-baked and the NEG vacuum activated. The NEG performance, from the point of view of secondary electron yield, has been re-established and is well below the electron multipacting threshold. However, all the uncoated parts present in these areas have lost the effect of their previously vacuum cleaning and scrubbing; thus needing a further time for the conditioning. As described in [18], the decrease in secondary electron yield of vacuum surfaces already scrubbed results much faster than an as-received surface. For this reason no scrubbing run should be foreseen for an operation at 50 ns bunch spacing. When the number of bunches is increased in the LHC, during the commissioning period of the machine, it is important to keep the bunch intensity as high as possible ($>1.2 \cdot 10^{11}$ p/b) so as to accelerate the re-cleaning of these surfaces during this period of time. Moreover, the presence of multipacting suppressor solenoids would ensure keeping the pressure rises acceptable for the physic run. Finally, during the commissioning period the vacuum interlock level could be increased up to $1.0 \cdot 10^{-6}$ mbar so as to not produce beam dumps due to triggering of a vacuum interlock.

2) Operation with 25 ns bunch spacing

The MD development studies performed in October and November 2011 with 25 ns confirmed the expected important electron cloud effect with heat deposition in the beam screen of all the cryogenic area of the LHC (~24 km). For an operation with 25 ns, a dedicated scrubbing run should be defined and planned. Furthermore, in such a case, a bunch intensity higher than the multipacting threshold ($\sim 1 \cdot 10^{11}$ p/b) should always be used. Vacuum pressure interlock could be increased up to $1.0 \cdot 10^{-6}$ mbar so as to increase the beam current without having beam dump.

Regarding the synchrotron radiation effect, if the LHC operates with 50 ns bunch spacing, no performance limitations are expected. In case the bunch spacing is reduced to 25 ns, thus opening the possibility to reach the nominal beam current, the accumulated photon dose in the arc will be $\sim 7\ 10^{23}$ ph/m *i.e.* one order of magnitude larger than at present and the achieved pressure at the arc extremity will be a few 10^{-10} mbar.

The pressure spikes observed during 20111, in LSS2 and LSS8, were analysed and inferred to beam heating. Following impedance experts recommendations, it was decided to modify the present design of the RF fingers and add ferrite pieces so as to absorb possible HOM trapped in the bellow module.

Temperature increase and gas desorption in the MKI, TDI and TCP collimators must be controlled during each physic fill and a detailed analysis of the NEG saturation level should be carried out in order to anticipate and foresee possible activities that could be performed during technical stops such as partial bake-outs and NEG vacuum activations.

The CMS pressure excursion registered during the physic run in 2011, due to a non-conform installation of the RF insert at 18 m right of the IP, is fixed. The area concerned was re-baked and the NEG coating activated. During the 2012 physic run pressure increase should no longer be registered in this location.

REFERENCES

[1] F. Ruggiero *et al.*, LHC Project Report 188, 1998.
[2] J.M. Jimenez *et al.*, LHC Project Report 632, 2003.
[3] G. Bregliozzi *et al.*, IPAC11 Proceeding, 2011,
[4] A. Rossi *et al.*, LHC Project Report 674, 2003.
[5] O. Dominguez *et al.*, IPAC11, 2011.
[6] G. Rumolo *et al.*, IPAC11, 2011.
[7] F. Zimmermann, LHC Project Note 201, 1999.
[8] G. Rumolo *et al.*, these proceedings.
[9] O. Gröbner, CAS 1999, CERN 99-05, CERN, 1999.
[10] E. Metral, F. Caspers, B. Salvant, J-L Nougaret, private communication.
[11] V. Baglin, ECR, EDMS document 1179000.
[12] B. Salvant *et al.*, these proceedings.
[13] G. Bregliozzi, EDMS document 1094561.
[14] G. Schneider *et al.*, EDMS document 1179993.
[15] G. Bregliozzi *et al.*, EDMS document 1179906.
[16] G. Bregliozzi *et al.*, EDMS document 1183364.
[17] D. Macina, ECR, EDMS document 1153295.
[18] J. M. Jimenez *et al.*, LHC Project Report 632, 2002.